energies

MDPI

Article

Economic and Environmental Analysis of Incorporating Geothermal District Heating System Combined with Radiant Floor Heating for Building Heat Supply in Sarein, Iran Using Building Information Modeling (BIM)

Atefeh Abbaspour, Hossein Yousefi *, Alireza Aslani and Younes Noorollahi

Department of Renewable Energies and Environment, Faculty of New Sciences and Technologies, University of Tehran, Tehran 14179-35840, Iran

* Correspondence: hosseinyousefi@ut.ac.ir

Abstract: Despite the considerable breakthrough in district heating systems (DHS) globally, there is not yet any policy on developing this technology in Iran. This country has a high range of energy demand, while renewable energies play a minor role in its energy supply chain. Furthermore, the world is going through a transition towards renewable resources, which currently consist of only 10% of the total energy mix. As the first contribution in this area, this paper aims to design a 100% renewable DHS integrated with radiant floor heating for a group of residential buildings in Sarein, Iran. Moreover, the literature proposes a novel approach for combining geothermal energy and Municipal Solid Waste (MSW) to achieve a 100% renewable energy system. Building Information Modeling (BIM) is used for thermal analysis by 3D designing the buildings in SketchUp and OpenStudio and simulating the heat load in EnergyPlus. Three scenarios are presented to better compare the DHS with the decentralized heating system regarding fuel consumption, as well as environmental and economic aspects. The town's existing heating system that consumes natural gas for both space heating and hot water demand is referred to as the IHS-G scenario. The DHS-G scenario represents an 87% renewable DHS system, working with natural gas and geothermal energy, while the DHS-MSW scenario is a 100% renewable system, consuming both geothermal energy and Municipal Solid Waste (MSW). Finally, findings suggest that DHS-MSW and DHS-G scenarios reduce the annual energy consumption of buildings by about 595 and 33 toes, respectively. Hence, the greenhouse gas effect will alleviate by mitigating the emission of 1403 and 1339 tons of CO_2-eq./year, respectively. Moreover, exporting the extra natural gas through both LNG and pipeline provides about 26 million and 28 million USD/year revenue in DHS-G and DHS-MSW scenarios.

Keywords: district heating system; radiant floor heating; EnergyPlus; natural gas; municipal solid waste; CO_2 mitigation

Citation: Abbaspour, A.; Yousefi, H.; Aslani, A.; Noorollahi, Y. Economic and Environmental Analysis of Incorporating Geothermal District Heating System Combined with Radiant Floor Heating for Building Heat Supply in Sarein, Iran Using Building Information Modeling (BIM). *Energies* **2022**, *15*, 8914. https://doi.org/10.3390/en15238914

Academic Editor: Antonio Rosato

Received: 29 September 2022
Accepted: 21 November 2022
Published: 25 November 2022

1. Introduction

The rapid growth of the world population and massive changes in lifestyle have substantially increased the energy demand and compounded the energy supply problem. About half of the global energy consumption is related to the heating industry sector [1]. The share of renewable technologies in the global energy mix is only about 10%, and a large proportion of the energy demand is still supplied from fossil fuels [2]. Global CO_2 emissions have increased more than twice from 1973 to 2018 [2]. The formulation of new policies in recent decades has paved the way to increase the share of energy-efficient and renewable technologies in the global energy mix. According to the Sustainable Development Scenario (SDS), the sale of low-carbon and clean heating technologies, such as district heating and renewable energy systems, should increase by more than half of the existing figure by 2030 [2]. The main factors that lead the new global policies toward energy transition and

diminish fossil fuel consumption over time are 1—Increasing the amount of CO_2 emission due to the combustion of fossil fuels and thus leading to anthropogenic global warming; 2—limitedness of the amount of fossil fuel. Thereby, by developing renewable-based technologies worldwide, an infinite energy source is harnessed, and the pace of global warming slows down.

Iran has one of the world's most significant oil and natural gas resources and is a founder member of OPEC (Organization of the Petroleum Exporting Countries). In this country, most of the domestic energy demand is supplied by these fossil fuels, and the share of other technologies is insignificant. Figure 1 shows a comparison between the amounts of supplied energy by various sources between 1990 and 2018. As per this figure, the consumption of natural gas has gradually increased in recent years as a result of the policy to expand the distribution grid and provide about 90% of households with natural gas [3]. Overall, 29% of the natural gas is used for space heating, while non-petrochemical and petrochemical industries, reinjection, and transportation are the further large consumers of natural gas in Iran [3]. The energy consumption rate is increasing rapidly in Iran due to population growth, subsidized supply of fossil fuel, and urbanization. This situation makes the country face challenges toward the sustainable development targets and ability to satisfy the future energy demand [4–6]. To alleviate the issue, the government plans to increase the share of renewable and energy-efficient technologies in the energy mix to achieve sustainable development goals and mitigate GHG emissions under the Paris Climate Agreement. Even though the country suffers from a long-lasting drought, hydropower has the largest share in Iran's energy sector among renewable energies, which has also been used in various countries worldwide for power generation on small [7,8] and large scales. However, there is a great opportunity for the government to exploit the high potential of solar, wind, and geothermal energy. In this regard, many domestic and foreign investors are recently working on projects to develop renewable technologies in this country [3].

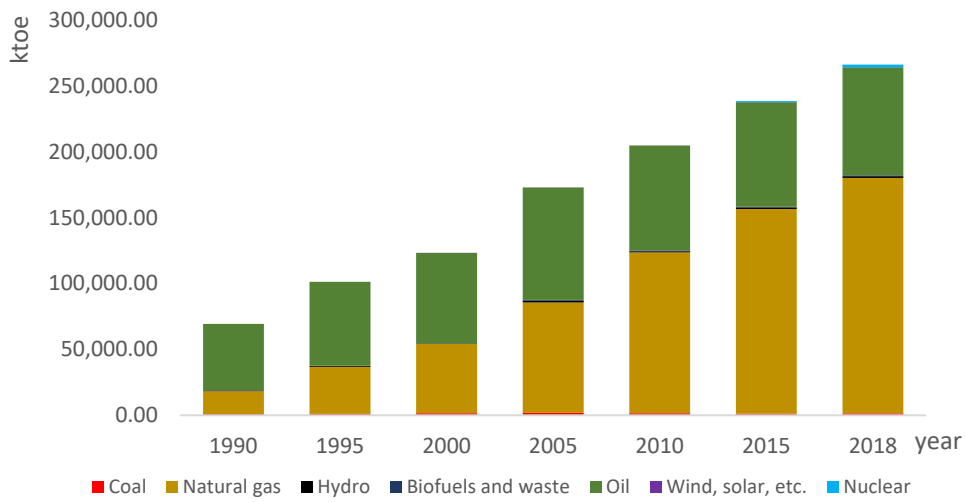

Figure 1. Comparison of supplied energy by various sources, 1990–2018 [9].

Generally, energy-efficient technologies are referred to as technologies operating efficiently, leading to lower energy consumption and thus energy-saving, which links to multiple economic, environmental, and social benefits. According to the IEA report [2], the residential sector accounts for 20% of the world's total final energy consumption, and about half of this figure is related to space heating. Hence, by developing the technologies for heating residential buildings, the countries' energy efficiency will be improved. There are various approaches toward this goal relating to either buildings' envelope as material, insulation, glazing, or heat supply system [10]. Generally, the buildings' heating demand (space heating and hot water) is supplied using decentralized and centralized heating systems. The utilization of renewable energies as heat sources and the improvement of in-

struments' efficiency has ramped up the efficiency in both types of systems. The centralized or so-called "district heating systems" (DHS) heat a group of buildings by a centralized heat generation unit. Regardless of their higher initial cost, they have many benefits over the latter system. Some of these benefits, which have conducted the governments to implement these systems rather than the decentralized ones, include higher flexibility of heat sources, lower fuel consumption, higher safety, and GHG emission reduction, especially when integrated with renewable energies [11]. Considering the high energy intensity and low energy efficiency in Iran, replacing the decentralized heating system with the DHS is a rational solution to fix these problems in this country which is investigated in this study.

Designing heating systems has been a deep-rooted action in history. In 1745, William Cook used steam piping to heat his house in Manchester and demonstrated that such a system could heat the buildings [12]. This action is considered the first attempt to heat a group of buildings with a single heat source. However, the first DHS was devised by American mechanical and hydraulic engineer Birdsill Holly in 1876 [12]. By the year 1930, steam had been used as an energy carrier in DHS, but it escalated the risk of explosions and caused substantial heat losses [13]. In the second generation of the DHS, pressurized hot water was used as a working fluid, and other components such as tube and shell heat exchangers and material-intensive heavy valves were also employed. The system had poor quality and lacked a heat demand control system but could improve fuel-saving [13]. In the 1970s, the third generation of DHS was developed. The pressurized water was still used as the working fluid in this system, but the supply temperature was lower than the previous generation (below 100 °C). This system is the so-called "Scandinavian district heating technology" and has been used in many countries in Europe, the USA, Canada, and China [13]. This paper considers a Floor Heating System to increase the heating system's efficiency. This system is also called a "Radiation Heating System", which transfers the heat by radiation. This technology is an ancient method used in 500 BC, as the "Hypocaust" in ancient Greece and Rome. Furthermore, Koreans were using a method so-called "Ondol", meaning "hot stone", which had a similar function to the floor heating system [14]. After World War II, this method became very popular in the United States. Some of the installed systems in this country are still operating. In the 1950s, the production of polyethylene pipes began, and in 1968, German engineer Thomas Engel developed the PEX type of pipes [15]. The proper inlet temperature for the floor heating system is between 30–50 °C which is lower than other available heating systems working between 60–75 °C. Therefore, energy consumption will decrease by up to 40% [16].

Sarein is a small town in northwestern Iran with a cold climate wherein the heating season lasts most of the year. Despite the substantial geothermal resources and multiple hot springs, the town's heating demand is still supplied by a natural gas firing decentralized system. Generally, geothermal energy is utilized in two forms; 1—Direct use; and 2—Indirect use (which focuses on electricity generation by hot water) [17]. The direct use of geothermal energy is referred to as using the hot fluid exploited from geothermal resources without converting it to other forms of energy, such as electricity [17]. The only application of the hot springs and geothermal energy in Sarein is establishing the hot water swimming pools. Another direct application of this energy source, which is investigated in this study, can be space heating of residential buildings using the DHS, and therefore, taking a step toward energy-efficient and sustainable development and reducing GHG emissions. Harnessing the geothermal hot water for district heating has been conducted in several cold regions such as Iceland [18]. The geothermal district heating system of Iceland was commenced in 1930 on a small scale. The system was developed to such an extent that it now supplies the heating demand of Reykjavik and the surrounding community, which covers 58% of the total population of Iceland. Detailed characteristics of these geothermal fields are presented in Table 1. This utility in Iceland is the world's most significant geothermal district heating. Thanks to this low-carbon technology Reykjavik is one of the cleanest capitals worldwide, avoiding about 100 million tons of CO_2 from 1930–2006 [18]. Hot springs in Sarein bear a close resemblance to Iceland's ones in terms

of natural flow rate and temperature; therefore, the adoption of a similar strategy and development of a renewable-based DHS in this town can provide a considerable amount of energy-saving and CO_2 emission reductions.

Table 1. Characteristics of geothermal district heating fields in Iceland [18].

Geothermal DHS Field	Location	Hot Spring Natural Flow Rate (L/s)	Temperature (°C)	Population Covered
The Reykir–Reykjahlíð	Reykjavik	120 (after 34 wells drilled, 2000 L/s)	70–83 (after well drilled, 85–100)	187,000
The Laugarnes	Reykjavik	-	120–140	
The Elliðaár	Reykjavik	-	95–110	
The Akranes-Borgarnes	Akranes and Borgarnes	180	98–99	8550
The Hveragerði	Hveragerði	80–85	180	2300
The Stykkishólmur	Stykkishólmur	-	87	1100
The Þorlákshöfn	Þorlákshöfn	-	100–120	1600
The Hella–Hvolsvöllur	Hella and Hvolsvöllur	-	70–100	1500

This paper aims to evaluate the feasibility of implementing a renewable-based DHS combined with a radiant floor heating system in Sarein and highlight the energy, environmental, and economic benefits gained with the utilization of such technology for the supply of heating demand in town instead of traditional natural gas-firing decentralized heating system. The aim is to supply the designed system with local renewable energy sources such as hot springs and municipal solid waste (MSW). Using building information modeling (BIM), a residential block is simulated in the environments of SketchUp and OpenStudio to develop data-rich 3D building models. The building models are then used in EnergyPlus to calculate the heating demand of the residential block. Both traditional and designed systems are studied to supply the heating demand of the block. Scenario analysis is finally conducted to propose the most sustainable combination of components and technologies in order to meet the heating demand in this town.

2. Literature Review

In response to the energy supply problems that occurred after the oil crisis of the 1970s, many communities have reconsidered their policy towards the energy mix and raised the share of renewables, in particular biomass, in the energy supply in order to enhance the energy security which is the so-called "Energy Transition". More efficient technologies such as DHS also have been implemented in the urban areas in order to meet the heating demand of the residential sector. A majority of the implemented DHSs are fossil fuel firing. A considerable effort has been in recent years made to combine these systems with renewable technologies. In this context, Di Lucia and Ericsson [19] studied the possibility of fuel transition in the Swedish heating system. They investigated the development pathway of DHS from 1960–2011, focusing on energy resources. This study's primary objectives are 1—a description of the transition from oil consumption to biomass and other kinds of renewable energy; and 2—to explain the transition of energy supply. Different theories and approaches, mainly Multi-Level Perspective (MLP), were employed to achieve these purposes. Noussan et al. [20] simulated a biomass-based combined heat and power (CHP) unit coupled with thermal energy storage (TES) for a district heating system. This study is conducted in Turin, Italy, and a multi-criteria approach is applied to analyze the economic and environmental aspects. They reported that the TES would lead the system to higher efficiency, and the maximum efficiency would achieve in a specific volume of the TES.

Finland is a cold north European country with a well-developed DHS. Almost half of Finland's residential population lives in district-heating apartments, and industrial and public buildings also benefit from this system. Paiho and Saastamoinen [21] investigated Finnish district heating development between 2018–2023. They interviewed principal energy organizations to assess the challenges and proceedings required for achieving the

development. This paper underlined that the primary focus should be on hybrid systems and improving the correlation with consumers. Lund et al. [22] pointed out district heating development prospects and their function in Intelligent Energy Systems (IES) development. This study's primary focus is on the next generation of DHS that can affect the future of the world's energy sector. Pan et al. [23] analyzed the performance of an existing district heating system located in London with an annual thermal load of 50,000 MWh in 2012. They evaluated refurbishment pathways in order to lower the operation cost and environmental impacts of the DHS. Lidberg et al. [24] studied the refurbishment of existing multi-family buildings in Sweden within various district heating systems to improve the beneficial environmental impacts. They proposed four scenarios for that purpose and concluded that reducing electricity usage is more critical than heat demand.

As mentioned earlier, the current energy policies guide the future of energy to maximize renewable's share. So in the fourth generation of the district heating system, heat supply will be accomplished through renewable energy. Pinto and da Graça [25] proposed two energy-efficient methods for supplying the heating demand of a group of residential buildings in the Netherlands; either refurbishing the existing buildings or developing a direct geothermal district heating system (GDHS). The results revealed that implementing district heating requires more initial cost, but it has the lowest environmental impact. Gunnlaugsson and Ívarsson [18] reported an overview of existing geothermal district heating fields in Iceland and their characteristics. Accordingly, these district heating systems were able to meet the heating demand of about 58% of Iceland's population. Yousefi et al. [26] studied geothermal fields' direct uses, such as developing district heating systems, greenhouses, and food processing in Meshkinshahr, Iran. Yildirim and Gökçen [27] modeled a low-temperature geothermal district heating system for a university campus in Turkey and compared its performance with the fossil fuel-based heating system in case of indoor air temperature and operational cost. In another study [28], Yildirim et al. designed an optimized piping network for the mentioned district heating and studied it in terms of cost and design parameters. Blázquez et al. [29] presented three different geothermal district heating, supplying both electricity and heating for a case study in Spain, and compared it with the traditional system from economic and environmental points of view. Stegnar et al. [30] introduced a framework to identify the potential shallow geothermal fields for individual and district heating systems in Slovenia. Chen et al. [31] designed a hybrid district heating system consisting of a geothermal heat pump and solar collectors and evaluated the sustainability and cost savings of the proposed system.

Kavian et al. [32] proposed a district heating system in Iran, working with geothermal hot spring heat pumps and using solar collectors as a supplementary heat source. They also investigated this system's energy performance and economic feasibility.

Dahash et al. [33] detailed a solar district heating system (SDHS) with seasonal thermal energy storage (STES). This study's main focus was on tank thermal energy storage (TTES) and pitted thermal energy storage (PTES) to store the hot water heated by solar energy. Renaldi and Friedrich [34] exerted a simulated model to study the performance of an SDHS with STES in Britain. This technology's feasibility study determined that it can be implemented but will have low technical performance. Furthermore, systematic analysis of the impact of system components on its performance indicated that not only solar energy supply and heat demand should be balanced, but also the appropriate size of the storage is required. They also concluded that this system could be implemented in mid to high latitudes. Ciapała et al. [35] studied wind power's performance as the peak energy source in a geothermal district heating system in Warsaw, Poland, and the results showed that wind energy could be a suitable complement for the geothermal heating system. Koch and Gaderer [36] investigated the techno-economic potential of the biomass-based plants combined with district heating, including thermal storage and PtH (Power-to-Heat) components. PtH is a technology that uses electricity to produce heat, such as heat pumps or electric boilers. Utilizing these technologies would promote the power supply security and affordability of the system.

The floor heating system is a heat distribution technology inside the buildings integrated into the district heating system in the current paper. This system has been studied in various research. Rastegarpor et al. [37] examined the impact of applying different energy storage types on system efficiency in a floor heating system operating through a heat pump. They improved the performance of building energy resources management systems by employing the Distributed Model Predictive Control (DMPC) method. Zhou and He [38] studied a low-temperature floor heating system due to different heat storage materials such as sand and Phase Change Materials (PCM) and different heating pipes such as Polyethylene coils and capillary mats. The inferred results indicated that the uniform temperature profile and a shorter time to attain a specific temperature would achieve by applying a capillary mat. Additionally, PCM would store the heat two times longer than the sand. As a result, a combination of capillary mat and PCM in-floor heating systems will promote the heating system's efficiency. According to Østergaard et al. [39], the transition of fossil fuel-based DHS to biomass-fired in small-scale district heating systems would not be appropriate for all regions due to constraints of biomass availability and utilizing biomass for superior goals. Table 2 summarizes the studies about district heating systems and floor heating systems reviewed in this section.

Table 2. Summary of investigated studies in the literature review (● = Yes).

Reference	Location	District Heating System						Floor Heating System
			Analysis			Main Objective		
		Energy Source	Environmental	Economic	Technical	Analyzing an Existing DHS	Developing New DHS	Energy Transition	
Di Lucia and Ericsson [19]	Sweden	Biomass			●			●	
Østergaard et al. [39]	Denmark	Biomass		●				●	
Paiho and Saastamoinen [21]	Finland	-					●		
Lund et al. [13]	Denmark	Renewable			●		●		
Pan et al. [23]	Britain	Natural gas	●	●	●	●			
Pinto and da Graça [25]	Netherlands	Geothermal		●			●		
Gunnlaugsson and Ívarsson [18]	Iceland	Geothermal	●			●			
Yousefi et al. [26]	Iran	Geothermal	●	●	●		●		
Yildirim and Gökçen [27]	Turkey	Geothermal			●		●		
Yildirim et al. [28]	Turkey	Geothermal		●	●		●		
Blázquez et al. [29]	Spain	Geothermal	●	●			●		
Stegnar et al. [30]	Slovenia	Geothermal		●	●		●		
Chen et al. [31]	China	Geothermal-solar	●	●			●		
Kaviani et al. [32]	Iran	Geothermal-solar		●	●		●		
Lidberg et al. [24]	Sweden	Biofuel-MSW-fossil fuel	●		●		●		
Dahash et al. [33]	Austria	Solar			●	●			
Renaldi and Friedrich [34]	Britain	Solar		●	●		●		
Ciapała et al. [35]	Poland	Geothermal-wind			●		●		
Noussan et al. [20]	Italy	Biomass		●	●	●			
Koch and Gaderer [36]	Germany	Biomass		●	●		●		
Rastegarpor et al. [37]	Italy								●
Zhou and He [38]	China								●

3. Case Study, Sarein County

"Sabalan" is the third highest mountain in Iran at 4811 m in elevation and an inactive volcano with a permanent lake at its summit. It is located northwest of Iran, with many cities and villages around it. There are numerous hot springs around the slopes of Sabalan, with the main concentration in Sarein County. This town has one of the most significant geothermal energy resources in Iran that can be utilized for not only bathing and swimming but also for heating the buildings. Figure 2 illustrates the location of Sarein in Ardabil province. Sarein has a cold and sub-humid climate with cold winters and mild summers. According to the meteorology data of the Ardabil province, obtained from the Meteorological Organization of Iran, Figure 3 shows the average monthly dry bulb

temperature of Sarein in a typical year based on the period of record from 1997 to 2017 (Typical Meteorological Year, TMY). As per this figure, heating is required in most parts of the year, and therefore, improvement of heating systems can result in a considerable reduction in the energy consumption of buildings in this town.

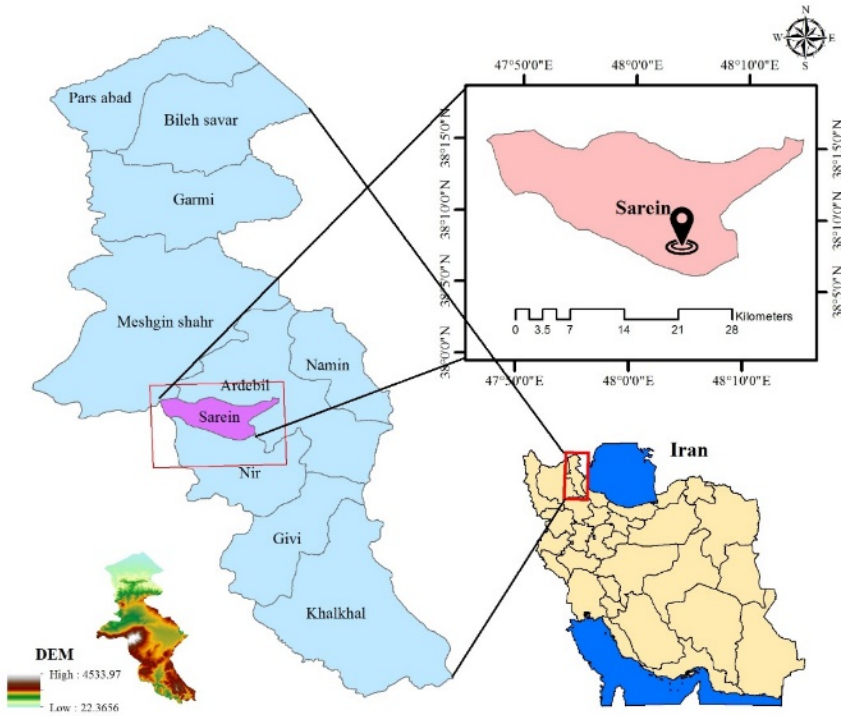

Figure 2. Location of Sarein in Ardebil province.

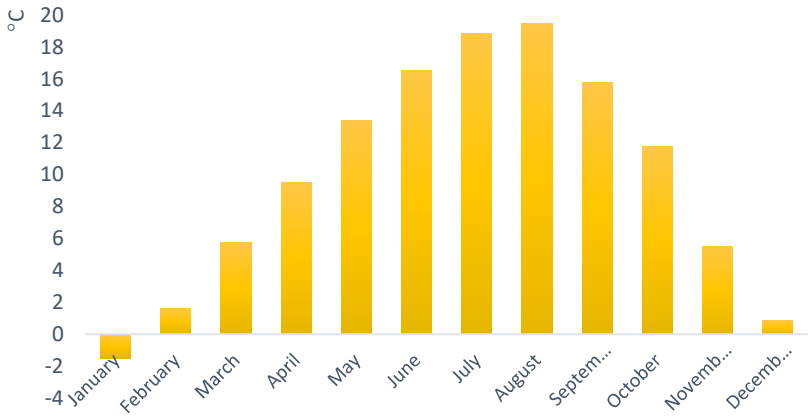

Figure 3. The average monthly dry bulb temperature of Sarein in a typical year.

There are nine main hot springs in Sarein. Characteristics of Sarein's hot springs are presented in Table 3 [40]. According to the table, Gavmishgoli hot spring has the highest flow rate and temperature. Thus, this study considers the characteristic of this hot spring in the modeling.

Table 3. Characteristics of hot springs in Sarein.

Spring	Flow Rate (kg/s)	Temp. (°C)	Capacity (MWt)
Sabalan	50	46	4.6
Gavmishgoli	140	47	12.89
others	26.5	42.8	2.31

4. Methodology

There are three main stages in this study 1—Investigating the study area from the renewable energy resources and meteorology points of view; 2—Simulation of the community using BIM; 3—Analyzing the results, proposing scenarios, and determining the appropriate path concerning the paper's objections. Figure 4 illustrates an overview of the study process. Considering the information given in the previous section, the heat demand in Sarein can be supplied by its natural renewable resources, such as hot springs. The temperature and flow rate of the Gavmishgoli hot spring is suitable for this purpose, and they can be utilized in a geothermal district heating system. Another renewable resource that can be utilized in the heating system of this town is municipal solid waste (MSW). In this study, a group of residential buildings is considered as the case study. The graphical design of case studies is conducted by the building information modeling (BIM) tool using SketchUp and OpenStudio software. The BIM models are then exported to a building energy simulation (BES) tool, EnergyPlus, in order to thermal analyze the buildings and determine their hourly space heating and hot water demand throughout the year. Recently, BIM tools have been widely used by architects and engineers to enhance a building's thermal performance, thus improving energy efficiency and sustainability in the building sector. BIM provides the opportunity to detect energy-saving opportunities in buildings' orientation, construction, material, human activities, and equipment in the initial design stages. Therefore, using BIM will lead to a significant amount of energy and time-saving. In this paper, the BIM model is created by storing buildings' envelope, material, orientation, infiltration, and occupancy [41]. The simulation procedure is detailed in the following section of the paper. Simulation results have been calibrated by comparing them with the results of other experiments [42,43]. After simulating the buildings, three different scenarios involving individual and centralized heating systems are presented to meet the buildings' heating demand, and their environmental impacts and economic benefits will be evaluated. Furthermore, a radiant floor heating system, operating at low temperatures (30–50 °C), is applied to distribute the heat inside the buildings to achieve a 100% renewable system.

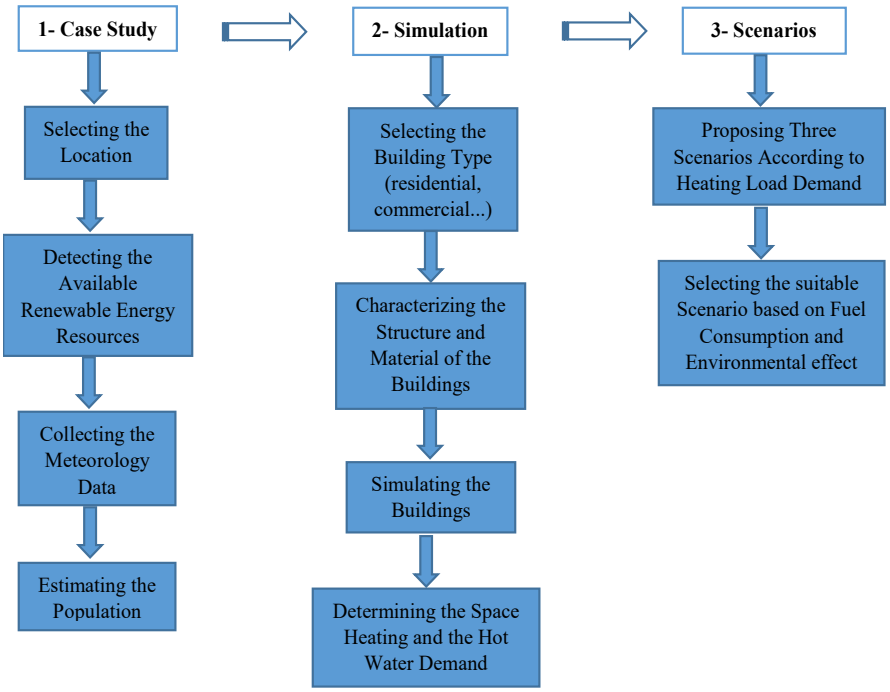

Figure 4. Overview of the three stages of the study.

5. Thermal Simulation

Before designing a heating system, the heating demand of buildings should be specified to determine the heat generation unit's capacity. Various types of simulation tools have been developed to facilitate this goal. Some tools provide the building's geometric and graphical design; known as BIM tools, such as SketchUp and Revit, and others are used for energy simulation and analysis; known as building energy simulation (BES) tools, such as EnergyPlus and eQUEST [41]. In this study, three simulation tools, including EnergyPlus, SketchUp, and OpenStudio, are used to simulate a group of buildings in Sarein. EnergyPlus is a console-based program that reads and writes only text files that were developed by the Department of Energy (DOE), USA. EnergyPlus does not involve a visual interface for graphical design; therefore, SketchUp is used as the interface to provide 3D models of buildings. OpenStudio is another interface for EnergyPlus that is utilized as a SketchUp plug-in.

The simulation has three steps. Figure 5 illustrates the simulation procedure in this study. First, the buildings' geometry, thermal zones, and orientation are modeled in SketchUp. Table 4 presents the characteristics of buildings modeled in SketchUp. Figure 6 illustrates the final 3D model of the buildings which were used for the simulation. According to this table, the population of the community is roughly 190 people. Southern and Northern orientation receives the maximum and minimum solar radiation, respectively, which affects the buildings' solar thermal gain. Second, the 3D models are exported to OpenStudio to specify the buildings' material, construction, and construction sets. An insulation layer is implemented to improve the buildings' thermal performance in the construction of walls, floors, and roofs, and two glazing layers with air fill are considered for the windows. Table 5 represents the characteristics of constructions inputted in OpenStudio. In the last step, the building spatial information modeled by the latter programs is exported to EnergyPlus as an 'idf' file. In EnergyPlus, the weather data of Sarein and the output of SketchUp and OpenStudio are used for buildings' energy simulation. Furthermore, as the coldest and warmest days of the year, a winter and summer design day is defined in EnergyPlus to determine the highest and lowest heat demands during a year. The data of winter and summer design days of most cities are available in the EnergyPlus weather data library [44]. Table 6 shows the characteristics of the winter design day used in the simulations. Note that according to Table 6, the summer design day's temperature is higher than the heating setpoint, and, therefore, it is not considered in the simulation. Other inputs in EnergyPlus include zone infiltration, occupancy, lighting, and heating and cooling thermostat schedules.

Table 4. Characteristics of the buildings modeled in SketchUp.

Building	Total Area (m^2)	Heated Area (m^2)	Building Residential Story	S/V Ratio (1/m)	Number of Building in Community	No of Occupants	Orientation
A	150	137	4	0.47	5	70	Southern
B	90	72	3	0.58	4	40	Western
C	180	160	3	0.48	6	80	Northern

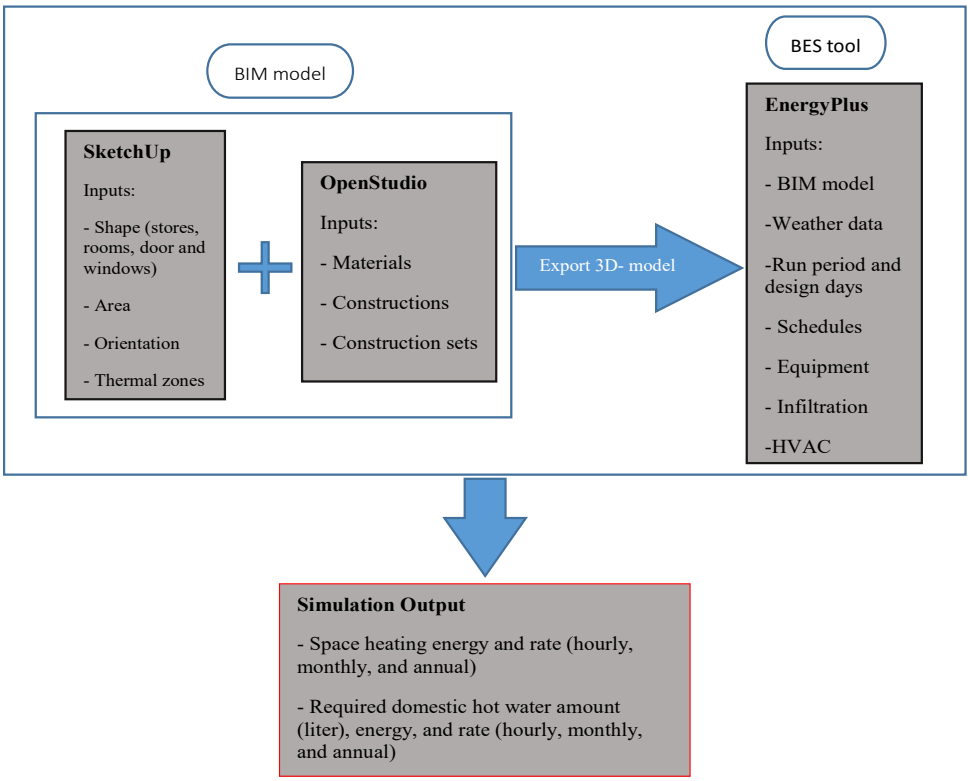

Figure 5. The simulation procedure in SketchUp, OpenStudio, and EnergyPlus.

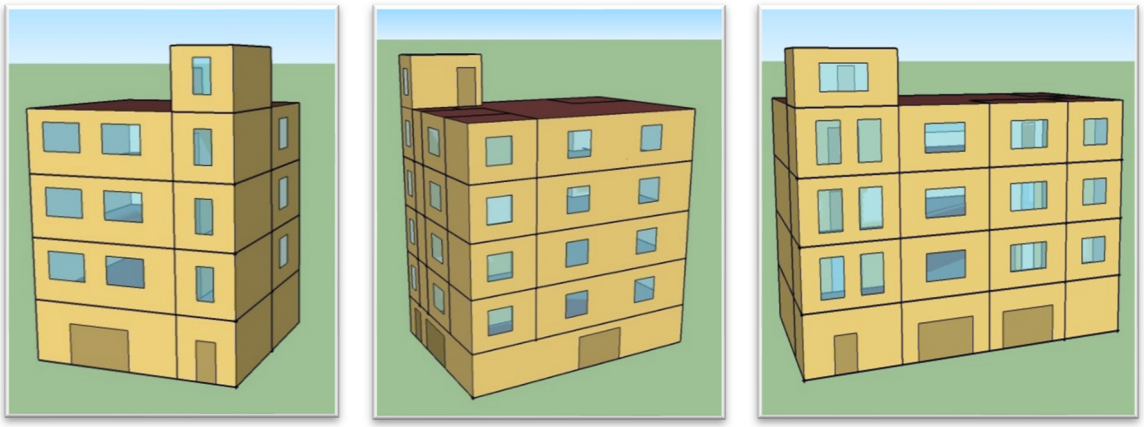

Figure 6. Three-dimensional model of the buildings in SketchUp. (Left to right: Building A, B, and C).

Table 5. Input construction of the buildings in OpenStudio.

Construction	Thermal Conductance (W/m^2·k)	Outer Solar Absorptance
Exterior Wall	0.4728	0.92
Interior Wall	3.664	0.4
Roof	0.4922	0.7
Ground	3.153	0.65
Ceiling	0.4769	0.7
floor	0.4769	0.4
Exterior Door	56,600	0.7
Interior Door	5.906	0.5

	Thermal Conductance (W/m^2·k)	Solar Heat Gain Coefficient (SHGC)	Visible Transmittance (VT)
Windows	3.7	0.757	0.804

Table 6. Parameters of the design days in EnergyPlus.

Month	Day of Month	Max. Dry-Bulb Temperature (°C)	Wet-Bulb at Max. Dry-Bulb (°C)	Wind Speed (m/s)	Wind Direction (deg.)
January	21	−10.9	−10.9	2.8	80
August	21	35.2	16.6	4.4	270

According to this study's objectives, the required outputs of simulation in EnergyPlus are buildings' space heating and domestic hot water (DHW) demands in Joule and Watt (hourly, monthly, and annual). The average heating demand in kW for the community in a typical year is represented in Figure 7. As per this figure, the heating demand during winter and summer varies between 15 kW and 131 kW, and the reason for the high disparity between the heating demands is the cold climate of the region. Figure 8 illustrates the total hourly heating demand of the community in a typical year. Figure 9 shows a comparison of heating demands in three different buildings. In these buildings, heating demand varies due to the different surface areas, the buildings' orientation, construction, and occupancy rates, but the minimum demand in all three occurs in July and August. Building C has the highest heating demand because its surface area is bigger than building A and B and has more occupants than other buildings. Furthermore, its orientation and most of the windows are north, which receives the least solar heat. On the other hand, building B has the smallest floor area and receives more solar radiation than building C. December, January, and February are the coldest months of the year in Sarein. Therefore, heat demand has the highest amounts in these months. Note that Sarein has a cold climate, and even in summer, heating is required on some days in all three buildings.

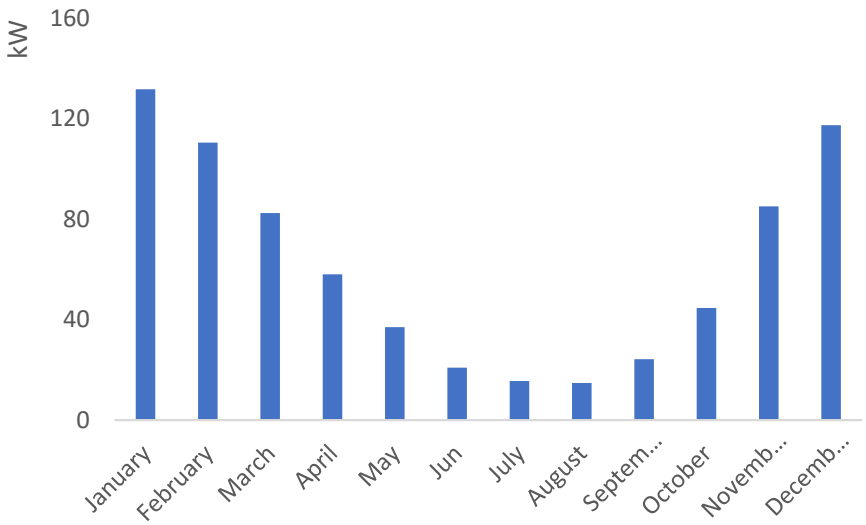

Figure 7. The average monthly heat demand of the group of buildings in a typical year.

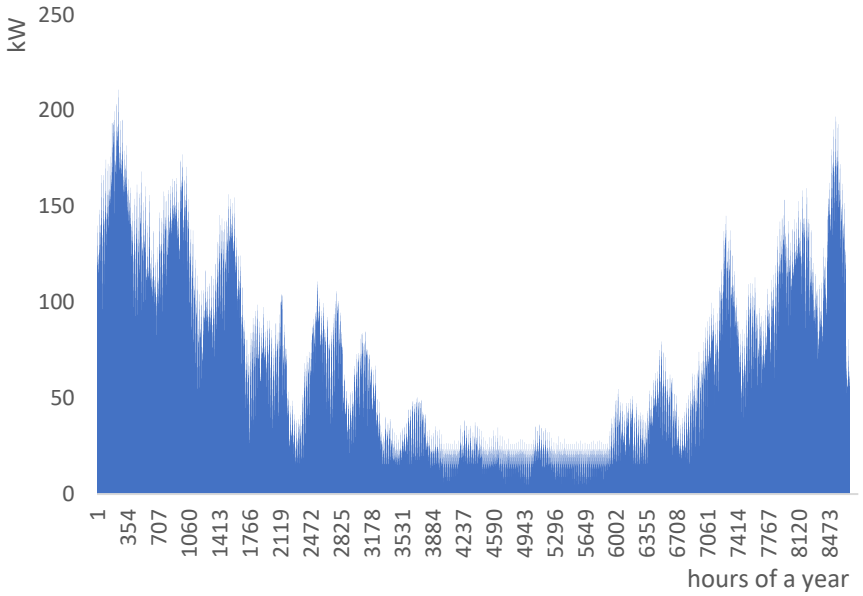

Figure 8. The total hourly heat demand of the group of buildings in a typical year.

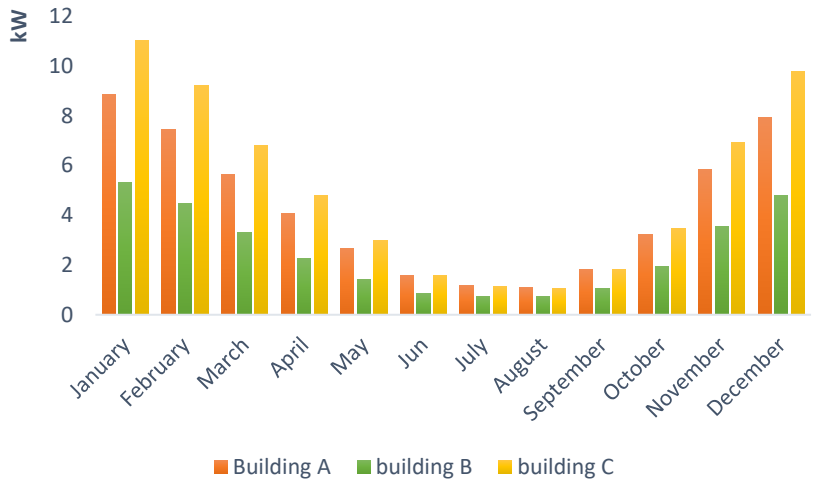

Figure 9. Comparison of heat demands in three different types of buildings.

6. Scenarios

This study focuses on comparing the existing heating system of Sarein with the district heating system. Thereby, three scenarios are defined and discussed regarding system equipment, natural gas consumption, CO_2 emission, and the obtained revenue. The scenarios are as follows:

1. Individual Heating System Scenario; reference scenario (IHS-G): The existing natural gas-piped decentralized system operates. Each apartment has an individual gas boiler supplying both space heating load (through the floor heating system) and domestic hot water (DHW). This system is not a renewable-based technology, and it is expected that it will have the highest amount of greenhouse gas (GHG) emission and natural gas consumption.
2. Gas-fired District Heating System Scenario (DHS-G): District heating as a centralized system is implemented and operates with a single gas boiler in a heat generation unit. This system only supplies the DHW, and hot spring geothermal water supplies the space heating demand by directly piping to buildings and circulating in a floor heating system. In this system, both renewable and fossil resources are utilized in a

district heating system, giving lower GHG emissions and natural gas consumption than the latter scenario.

3. MSW-fired District Heating System Scenario (DHS-MSW): This scenario presents a 100% renewable-based district heating system. The gas boiler in the previous scenario is replaced by an MSW-fired boiler, and the hot spring water supplies the space heating demand by directly piping and circulating water in a floor heating system. This system is the most energy-efficient technology, and local and renewable energy resources supply the whole heating demand. Thus, it is expected that GHG emissions and natural gas consumption will be the lowest amount in this scenario.

6.1. IHS-G Scenario

This system's main components are an individual gas boiler for each building unit and a floor heating system. A simple schematic diagram of the individual heating system applied in this scenario is illustrated in Figure 10. The boiler supplies the ambient heating and DHW load. Given the total thermal power (in kW), boiler capacity is calculated. The reliability factor of 1.1 is considered due to thermal losses. Therefore, the boiler's capacity can be calculated as follows:

$$P_{boiler}(\text{kW}) = (P_s(\text{kW}) + P_{DHW}(\text{kW})) \times 1.1 \quad (1)$$

where P_{boiler} is the boiler's capacity, P_s is ambient heating thermal power, P_{DHW} is domestic hot water thermal power, and 1.1 is the correction factor.

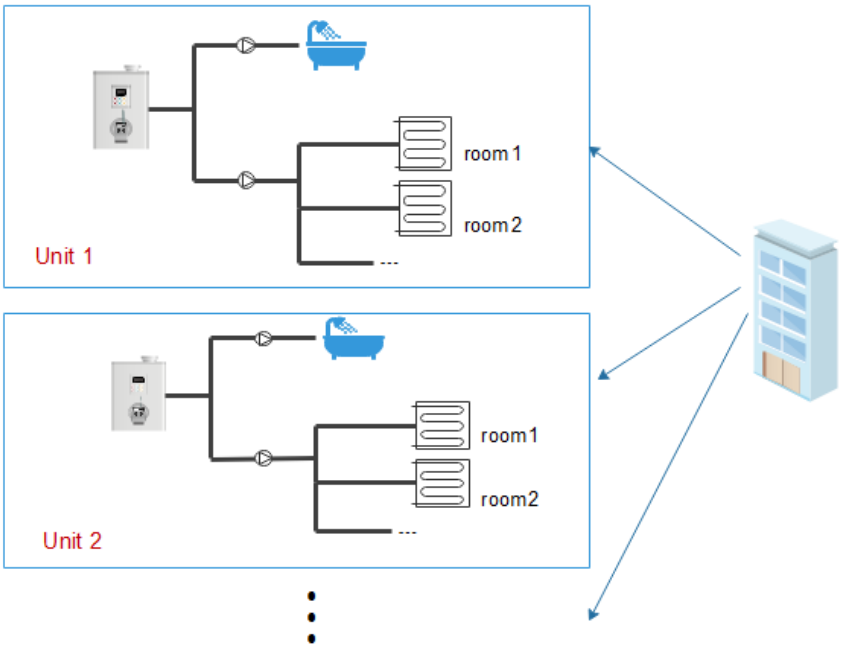

Figure 10. Simple diagram of the individual heating system in IHS-G Scenario.

According to the simulation results, the hourly and monthly values of P_s and P_{DHW} are available. However, to calculate the nominal boiler capacity, the peak load should be considered. Therefore, the heat load on winter design day is assumed as the peak load. A gas burner is a component of a boiler that provides heat by combustion of a fuel. The considered boiler in this scenario is a gas boiler that consumes natural gas. Thus, the natural gas consumption rate is calculated as:

$$C_{NG}(\text{m}^3/\text{s}) = \frac{P_{boiler}\ (\text{MW})}{HV(\text{MJ}/\text{m}^3) \times \eta} \quad (2)$$

where C_{NG} is natural gas consumption, HV is the heating value of natural gas (the HV of the available natural gas in Iran is 38 MJ/m^3 [19]) and η is the boiler's efficiency.

As aforementioned, a part of the boiler's output is piped to the floor heating system. The hot water is distributed through a manifold with various branches (depending on the surface's piping design). The boiler's inlet water, which is supplied by the municipal water system, is considered to be 10 °C. The maximum outlet temperature of DHW and floor heating is 60 °C and 45 °C, respectively, and the return water of the floor heating is 35 °C. The basis of the floor heating system design is analyzing the room-by-room heat losses that require precise data on the construction, lowest outdoor temperature, location, and infiltration rate. Inserting insulation in the construction of walls, ceilings, and floors can reduce the overall heat transfer coefficient (U) and the number of heat losses. The designed parameters of the floor heating system for each unit of buildings A, B, and C are shown in Table 7.

Table 7. Characteristics of floor heating system of the buildings.

Parameter	Building A	Building B	Building C
Total loop length (m)	790	381	808
Manifold trunk flow rate (L/h)	783	638	1349
Manifold trunk diameter (mm)	16	16	16
Floor heating pipe diameter (mm)	27	27	27
Number of branches	9	4	9
Average speed of flow in pipe (m/s)	0.36	0.37	0.26

In the end, the boiler's capacity and natural gas consumption on design day are calculated and demonstrated in Table 8.

Table 8. The capacity of the boiler and natural gas consumption in the buildings.

	Building A	Building B	Building C	Total Community
Capacity (kW)	17	10	20	-
Natural gas consumption in 24 h (m^3)	36	22	46	1812

6.2. DHS-G Scenario

In DHS-G and DHS-MSW scenarios, a district heating system is modeled, and a simplified diagram of it is illustrated in Figure 11. Considering the appropriate temperature of 60 °C for DHW, the hot spring water of 47 °C cannot be used for this purpose. Therefore, a gas boiler is implemented to heat the hot spring water to 72 °C for DHW. However, the hot spring's direct application is considered for the buildings' ambient heating, although it should pass through a water softener due to its chemical composition and hardness, which is corrosive toward standard materials. Then, the water will be directly piped to the community and heat the buildings through a floor heating system with the same character as in the first scenario. The outlet water of the boiler flows into a plate heat exchanger (HE). In an indirect distribution system, the HE is applied as the connection point between the heat generation unit and the consumers' distribution network. Therefore, the system's two parts are not directly connected, and any contamination in the system would not spread [45,46].

In this scenario, the boiler is gas-fired and modulating, which can operate in full and part loads. Generally, the part load capacity is considered 30% of the full load [47]. Recently, condensing boilers have been widely increased due to their superior efficiency and reduced fuel consumption. An additional condensing heat exchanger in these boilers can absorb the vapor's latent heat in the hot flue gases. Then, the vapor condenses into droplets and drains from the bottom of the boiler. This process increases the efficiency of the boiler by as much as 10–12% [48], and up to 110%, thermal efficiency based on lower heating value (LHV) and almost 99% on higher heating value (HHV) is achievable. Therefore, the considered boiler in this district heating system is a condensing gas boiler. The DHW consumption

of a sample household on a typical day in building A is shown in Figure 12. Accordingly, the maximum demand of DHW is at 8:00 a.m. Thus, the outlet flow rate of the boiler is calculated by:

$$Q\left(\frac{\mathrm{m}^3}{\mathrm{s}}\right) = \frac{P(\mathrm{kW})}{4200 \times \Delta T} \tag{3}$$

where Q is the flow rate, P is the boiler's capacity, ΔT is the temperature difference between the inlet/outlet flows of the boiler, and 4200 is the specific heat capacity of water in J/kg °C. According to Equation (3), assuming a constant value of capacity (P), increasing the ΔT leads to diminishing the flow rate. Notice that the boiler's outlet flow enters the heat exchanger, and thus, it indirectly heats the main flow, which is transferred to the community. Table 9 provides characteristics of the boiler designed for the district heating system.

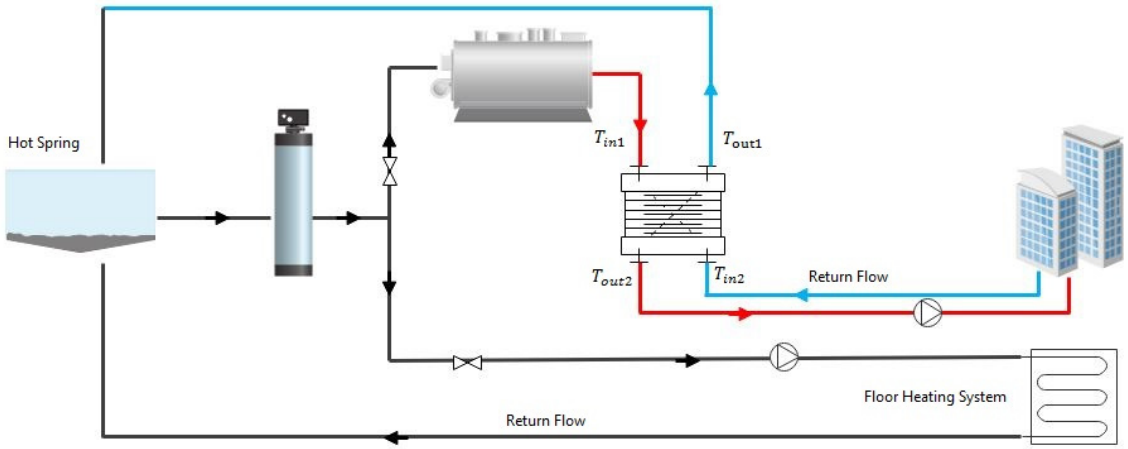

Figure 11. Simplified diagram of the DHS system in DHS-G scenario.

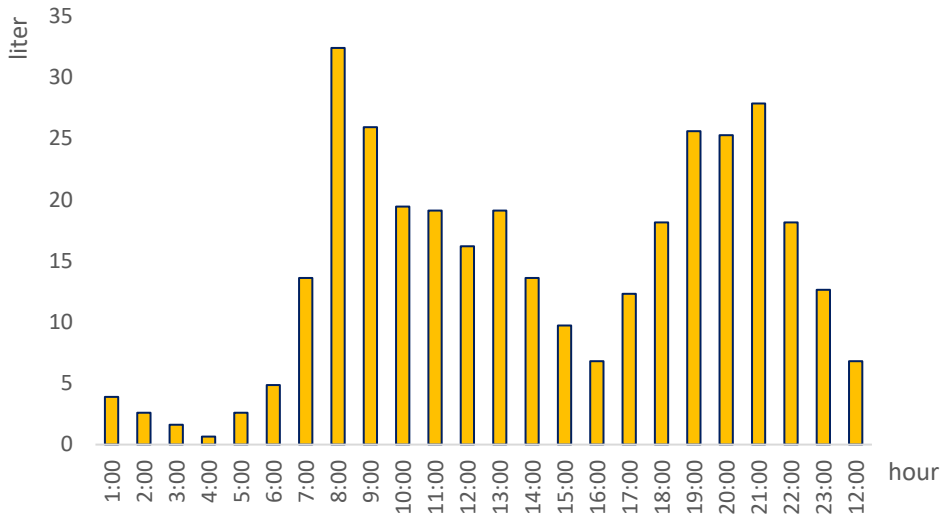

Figure 12. The DHW consumption of a sample household in Building A.

The proper type of heat exchanger for geothermal applications is generally a plate heat exchanger. Various corrosion-resistant alloys are used in plate heat exchangers' surface construction, but manufacturers commonly use 304 or 316 stainless steel as the primary material [49]. The principal parameter in selecting the heat exchanger is the heat transfer area which is calculated by the general equation of heat exchangers:

$$Q = U \times A \times LMTD \times C_f \tag{4}$$

where, Q is the heat load in W, U is overall heat transfer coefficient in W/m^2 °C, A is heat transfer area in m^2, $LMTD$ is the log mean temperature difference in °C, and C_f is the $LMTD$ correction factor (0.85–1.0 for most geothermal applications [49]). $LMTD$ is calculated by the following equation:

$$LMTD = \frac{\Delta T_1 - \Delta T_2}{\ln\left(\frac{\Delta T_1}{\Delta T_2}\right)}, \begin{cases} \Delta T_1 = T_{\text{out1}} - T_{in2} \\ \Delta T_2 = T_{in1} - T_{out2} \end{cases} \quad (5)$$

where, T_{in1}, T_{out1}, T_{in2} and T_{out2} are the inlet and outlet temperatures of fluid one and two, respectively. The overall heat transfer coefficient (U) is determined according to the data released by [49], which depicts the interconnection between the fouling factor, pressure drop, and the U. Table 10 shows the characteristic of the heat exchanger designed for the district heating system.

Table 9. The characteristics of the boiler in district heating system.

	Full Load	Part Load
Capacity (kW)	120	34
Inlet temp. (°C)	47	47
Outlet temp. (°C)	72	72
Efficiency (%)	92	96
Outlet flow rate (L/h)	4104	1152
Natural gas consumption in 24 h (m^3)	91	10

Table 10. Characteristics of the heat exchanger.

Plate Material	316 Stainless Steel
Overall heat transfer coefficient (W/m^2 °C)	5400
LMTD correction factor	1
Inlet and outlet temperature of the hot water (°C)	72–47
Inlet and outlet temperature of the cold water (°C)	38–68
Total heat transfer area (m^2)	3.6
The outlet flow rate in the full-load (L/h)	2975
The outlet flow rate in the part-load (L/h)	835

6.3. DHS-MSW Scenario

In this scenario, the district heating system's outline is the same as the DHS-G Scenario, but the boiler's fuel is municipal solid waste (MSW) instead of natural gas. Inasmuch as Sarein is a resort destination, it has higher per capita waste generation rates in comparison to the other cities of Iran. The utilization of MSW as the primary energy source for the DHS enhances the share of renewables in the energy mix on the one hand and alleviates waste deposition issues on the other hand. To this end, the amount of heat released by combustion of the MSW (heating value) should be determined and realize how much MSW is required to meet the community's heating demand. The higher and lower heating value of MSW is calculated by the following equations, respectively [50]:

$$\text{HHV}\left(\frac{\text{MJ}}{\text{kg}}\right) = 34.1\text{C} + 123.9\text{H} - 9.85\text{O} + 6.3\text{N} + 19.1\text{S} \quad (6)$$

$$\text{NHV}\left(\frac{\text{MJ}}{\text{kg}}\right) = \left(\text{HHV}\left(\frac{\text{MJ}}{\text{kg}}\right) - 21.92\text{H}\right)\left(1 - \frac{\text{MCWB}}{100}\right) - 0.02452\text{MCWB} \quad (7)$$

where, HHV and LHV are higher and lower heating values, respectively. C, H, O, N and S are weight% of carbon, hydrogen, oxygen, nitrogen, and sulfur in the MSW, respectively.

Moreover, MCWB is the Moisture Content Wet Basis which is calculated using the following equation [51]:

$$\text{MCWB} = \frac{W_{moisture}}{W_{tot}} \times 100 \quad (8)$$

where, $W_{moisture}$ and W_{tot} are the weight of moisture and total weight of MSW respectively.

There are two methods to analyze the chemical composition of MSW; proximate and ultimate analysis. The ultimate analysis used in this paper is conducted based on Tchobanoglous et al. [51]; the common data for the ultimate analysis of MSW and MCWB% are represented in Table 11.

Table 11. The common data for the ultimate analysis of MSW and MCWB% [51].

Waste Type	S (%)	N (%)	O (%)	H (%)	C (%)	Ash (%)	Moisture (%)
Plastic	-	-	22.8	7.2	60	10	2
Paper/Cardboard	0.2	0.3	44.5	5.8	43.2	5.5	5.5
Metal	-	0.1	4.3	0.6	4.5	90.5	3
Textile	0.2	2.2	40	6.4	48	3.2	10
Glass	-	0.1	0.4	0.1	0.5	98.9	2
Wood	0.1	0.2	42.7	6	49.5	1.5	20
Rubber	1.6	-	-	8.7	69.7	20	2
Leather	0.4	10	11.6	8	60	10	10
Dirt, sand, stone	0.2	0.5	2	3	26.3	68	8
Food waste	0.4	2.6	37.6	6.4	48	5	70

According to obtained data from the Municipality of Sarein, the total waste production in Sarein is around four tons per day, and the composition of the MSW in Sarein is as shown in Table 12.

Table 12. Composition of the MSW in Sarein.

Waste Type	Component %
Plastic	8.7
Paper/Cardboard	4.17
Metal	1.7
Textile	2.67
Glass	2.41
Wood	1.81
Rubber	1.3
Leather	0.81
Dirt, sand, stone	1
Food waste	75.22

Using Tables 11 and 12, the heating value of the MSW is calculated. The results reveal that the HHV and LHV of the MSW in Sarein are 24.05 MJ/kg and 10.31 MJ/kg, respectively. Moreover, the efficiency of the biomass boiler is presumed to be 0.85 [50]. Hence, by replacing the heating value of MSW with natural gas in Equation (2), about 176 kg/day MSW is needed to meet the heating demand of case studies.

7. Results

The proposed technologies are investigated from economic and environmental viewpoints in this section. Table 13 compares the rate of fuel consumption in the proposed scenarios. Accordingly, the DHS-MSW scenario is a 100% renewable and local system and can decrease the town's total natural gas consumption, leading to society's environmental and economic benefits.

Table 13. Natural gas and MSW consumption in proposed scenarios.

Scenario	Natural Gas Consumption per Year (toe)	MSW Consumption per Year (ton)	Share of Renewable Energy (%)
IHS-G	595	-	0
DHS-G	33	-	87
DHS-MSW	-	64.2	100

7.1. Environmental Aspect

Analyzing the environmental impact of fuel consumption in the systems requires calculating GHG emissions within the heat production process. Three main GHGs are Carbon dioxide (CO_2), Methane (CH_4), and Nitrous oxide (N_2O). The emission of each gas is converted to CO_2 equivalent (CO_2 eq.), based on their impact on global warming, so-called "Global Warming Potential" (GWP), to measure the total GHG emitted. In this study, the greenhouse effect of three gases in 100 years (GWP100) is considered as [50]:

$$1\ t\ CH_4 = 22\ t\ CO_2, \quad 1\ t\ N_2O = 310\ t\ CO_2$$

7.1.1. GHG Emission of MSW

The emission factor for collecting and transporting of MSW is 0.008 t CO_2 (eq.)/t MSW [52]. Table 14 shows the emission factor and average heating value of MSW [53].

Table 14. The emission factor and average heating value of MSW [53].

LHV	9–12 MJ/kg
CH_4 emission factor	0.2 g/ton MSW
N_2O emission factor	50 g/ton MSW

MSW incineration releases two types of carbon: fossil and biogenic carbon. Fossil carbon locks up in the atmosphere and causes the greenhouse effect, whereas biogenic carbon is part of an ecosystem cycle and absorbed by the plants in nature, which has no adverse effect on climate. Hence, to determine the CO_2 emitted by CO_2 incineration, just the amount of fossil carbon should be considered. The following equation has been proposed by the IPCC (Intergovernmental Panel on Climate Change) to calculate the CO_2 emission of MSW incineration [54]:

$$CE = \sum_i (SW_i \times dm_i \times CF_i \times FCF_i \times OF_i) \times \frac{44}{12} \quad (9)$$

where, CE is CO_2 emission of MSW incineration in kg CO_2/kg MSW, SW_i is the total (wet) amount of MSW type i in kg/kg MSW, dm_i is %dry matter content of MSW, CF_i is %carbon in dry matter, FCF_i is %fossil carbon in the total carbon, OF_i is the oxidation factor (presumed 100%) and $\frac{44}{12}$ is the conversion factor from C to CO_2. Fossil Carbon Fraction (FCF) is an index to determine the amount of fossil carbon in the total carbon content of MSW. In this study, the FCF index based on the data provided by [54] is used. Table 15 depicts the result of calculating CO_2 emission per day by MSW incineration.

Table 15. CO_2 emission per day by MSW incineration [54].

Waste Type	FCF (%)		SW (kg)	dm (%)	CF (%)	CO_2 Emission (kg/day)
	Default	Range				
Plastic	100	95–100	15.3	98	60	33
Paper/Cardboard	1	0–5	7.3	94.5	43.2	0.11
Metal [1]	-	-	3	97	4.5	-
Textile [2]	20	0–50	4.7	90	48	1.5
Glass [1]	-	-	4.2	98	0.5	-
Wood	0	0	3.2	80	49.5	0
Rubber and Leather	20	20	3.7	88	67	1.6
Food waste	-	-	132.4	30	48	-
others	100	50–100	0.4	-	-	-
Total	-	-	-	-	-	36.2

[1] There is a small amount of fossil carbon in metal and glass, but a significant amount of them does not burn in the incinerating process. [2] It is presumed that 40% of the textile is made up of synthetic fiber. Hence, using Tables 14 and 15, the total amount of GHG emission in the DSH-MSW scenario is determined, and the data are shown in Table 16.

7.1.2. GHG Emission of Natural Gas and Comparing the Scenarios

The emission factors per energy unit for natural gas combustion are represented in Table 17 [50]. Thus, the total GHG emitted in IHS-G and DHS-G scenarios can be calculated. Table 18 shows the GHG emission and greenhouse effect of the heating supply systems in the three scenarios, and a comparison of them is illustrated in Figure 13. According to the results, implementing the DHS-G and DHS-MSW scenarios instead of the existing system (IHS-G scenario) decreases the greenhouse effect up to 1338.7 tons CO_2 eq./year and 1403.2 ton CO_2 eq./year and has a positive impact on the global warming issue.

Table 16. The total amount of GHG emission in the DSH-MSW scenario.

	Amount of Emission (ton/year)	GWP	Greenhouse Effect (ton CO_2 eq./year)
CO_2	13.2	1	13.2
CH_4	0.000013	22	0.00029
N_2O	0.0032	310	0.992
Collecting and transport	-	-	0.512
Total	-	-	14.7

Table 17. The emission factors of natural gas [50].

GHG	Emission Factor (kg/GJ)
CO_2	56.1
CH_4	0.003
N_2O	0.001

Table 18. The GHG emission and the greenhouse effect of the three scenarios.

Scenario	CO_2 (ton/year)	CH_4 (ton/year)	N_2O (ton/year)	Greenhouse Effect (ton CO_2 eq./year)
IHS-G	1410	0.075	0.025	1417.9
DHS-G	78.7	0.0042	0.0014	79.2
DHS-MSW	13.2	0.000013	0.0032	14.7

7.2. Economic Aspect

According to the latest ratification by the ministry of petroleum in Iran in 2020, the price of natural gas varies according to the five climate type classifications and the range of monthly consumption in two groups of cold months (from November to April) and

warm months (from May to October) of the year. Considering this pricing, each cubic meter of natural gas in buildings A, B, and C in cold months costs 3864, 2208, and 4830 IRR, respectively, and in warm months is 3956, 2806, and 4301 IRR, respectively. Hence, by using the hourly data of heating energy demand and mentioned prices, the annual cost of natural gas consumption for each building is calculated. Moreover, the price of natural gas exports through LNG and pipeline is assumed to be 23 and 20 cents USD per cubic meter, respectively [55]. Considering that there is still no district heating system in Iran, the price of natural gas consumption in the DHS-G scenario is set at 1000 IRR per cubic meter, based on the price of industrial application. Table 19 represents the annual cost of natural gas for the consumers and the revenue of exporting the extra gas (due to implementing the scenarios in the community). Furthermore, Figure 14 illustrates the average monthly natural gas cost in every building.

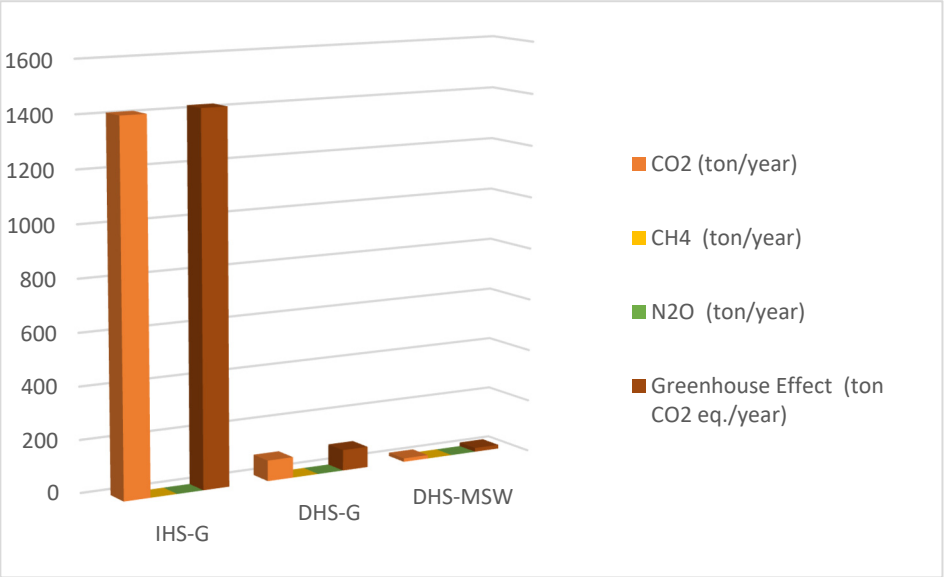

Figure 13. The comparison of GHG emission and greenhouse effect of the three scenarios.

Table 19. The annual cost of natural gas and the revenue of exporting the extra gas.

Scenario	The Annual Cost of Natural Gas Consumption (IRR)			Revenue of Exporting the Extra Natural Gas (USD)	
				LNG	Pipeline
IHS-G	Each unit of building A	Each unit of building B	Each unit of building C	0	0
	12,591,268	3,951,128	12,871,315		
DHS-G	36,865,000			14,363,845	12,490,300
DHS-MSW	0			15,211,740	13,227,600

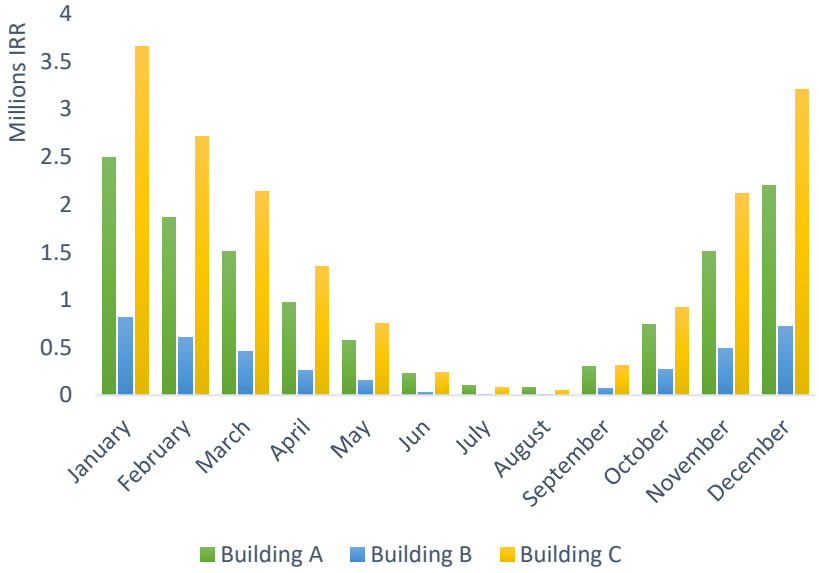

Figure 14. Comparison of the average monthly natural gas cost for consumers.

8. Discussion

As mentioned earlier, the world is going toward sustainable and renewable energy supply systems in all sectors, such as residential, industry, and transportation. Furthermore, energy-efficient technologies are developing and spreading rapidly in the market all over the world. The increasing greenhouse gas emissions and intensification of global warming due to human activities have forced policymakers and governments to legislate new policies toward sustainable development. Therefore, the more a technology is efficient and renewable-based, the more it will align with these policies. To this goal, this paper compared the energy, economic, and environmental performance of three heating systems to supply the heating demand of residential buildings.

In the first scenario, the individual fossil fuel-based technology was modeled, and the analysis showed that it is the worst system to supply the heating demand. In this system, the amount of annual natural gas consumption is 595 toes, which is very high compared to the two other scenarios, and based on the assumptions of this scenario, no excess natural gas remains to export and make revenue. The second scenario suggested a geothermal district heating system that consumes both natural gas and geothermal hot spring as energy resources. The principal part of residential heat demand is ambient heating, supplied by plumbing the hot spring water to the buildings in this scenario. Additionally, to reduce fossil fuel consumption and increase the system's efficiency, a floor heating system was designed to heat the buildings with a hot spring because this system works with low-temperature water and the hot spring's temperature was warm enough to use directly in this system. Moreover, a modulating condensing boiler, as an energy-efficient technology, was implemented in the district heating system to meet the buildings' domestic hot water demand. Therefore, the second scenario is more environmentally friendly than the latter; it consumes only 33 tons of natural gas per year, and there will be 562 tons of surplus natural gas annually, which makes 14 million USD annual revenue by exporting the gas through LNG. The last scenario was analogous to the second one in terms of space heating supply by hot spring, but it consumed municipal solid waste, rather than natural gas, in the heat generation unit of the district heating system, which made it a 100% renewable-based system: integrating the geothermal and MSW resources. There was no natural gas consumption in this system; thus, 595 tons of natural gas could be exported and make 15 million USD annually. Moreover, this system's environmental impact is the least, with a greenhouse gas effect of 14.7 tons CO_2 eq./year. Therefore, with the minor environmental disadvantages and most economic benefits, the third scenario is the most suitable system to supply the heating of a group of buildings in Sarein.

9. Conclusions

This study's main objective was to involve local and renewable energy resources to meet residential buildings' heat demand. In this regard, a renewable district heating system as a safe and environmental-friendly system was designed with focusing on heat generation units for a group of buildings in Sarein, Iran. To improve the buildings' efficiency, a BIM model was provided to simulate well-constructed and insulated buildings. These buildings were also presumed to be constructed close to the hot spring to diminish heat loss in the heat distribution network. The most important renewable energy resource of Sarein is geothermal energy combined with MSW to develop a 100% renewable heating system with environmental and economic benefits for the whole community. Considering a small community as the case study, the amount of solid waste was adequate for that, but more investigations are required to determine if it can meet the heat demand of the whole town in a more comprehensive district heating system. Furthermore, using solid waste in the heating supply will solve the problem of waste disposal. By far, there is no operating district heating system in Iran, so there is not any pricing for this type of heating. Therefore, in economic analysis, the price of natural gas consumption in industrial units was presumed to calculate the district heating's cost.

The exact heat loss calculations and distribution network's design were not provided in this paper which can be investigated in other studies. Moreover, in this study, the designed system only supplies heating. However, a combined heat and power (CHP) district system can be modeled by enhancing the heat generation unit and implementing thermal energy storage (TES) to produce heat and electricity simultaneously. Furthermore, in future studies, the district heating system can be integrated with other renewable resources, such as wind or solar energy, as peak load complements.

In conclusion, this paper's results reveal a possibility of alternating Sarein's existing heating system with better and more environmentally friendly solutions, a geothermal district heating system. In that way, the amount of fossil fuel usage and its negative impacts on the environment and global warming can be diminished. Meanwhile, the extra natural gas can be exported and assist in enhancing the economy of the country.

Author Contributions: Validation, Y.N.; Writing—original draft, A.A. (Atefeh Abbaspour); Writing—review & editing, A.A. (Alireza Aslani); Supervision, H.Y. All authors have read and agreed to the published version of the manuscript.

Funding: This research received no external funding.

Data Availability Statement: Not applicable.

Conflicts of Interest: The authors declare no conflict of interest.

References

1. Chomać-Pierzecka, E.; Kokiel, A.; Rogozińska-Mitrut, J.; Sobczak, A.; Soboń, D.; Stasiak, J. Hydropower in the Energy Market in Poland and the Baltic States in the Light of the Challenges of Sustainable Development—An Overview of the Current State and Development Potential. *Energies* **2022**, *15*, 7427. [CrossRef]
2. IEA. *Heating*; IEA: Paris, France, 2020.
3. Azadi, P.; Sarmadi, A.N.; Mahmoudzadeh, A.; Shirvani, T. *The Outlook for Natural Gas, Electricity, and Renewable Energy in Iran*; Stanford University: Stanford, CA, USA, 2017.
4. Yetano Roche, M.; Paetz, C.; Dienst, C. *Implementation of Nationally Determined Contributions—Islamic Republic of Iran Country Report*; Umweltbundesamt: Dessau-Roßlau, Germany, 2017.
5. Mohammadnejad, M.; Ghazvini, M.; Mahlia, T.M.I.; Andriyana, A. A review on energy scenario and sustainable energy in Iran. *Renew. Sustain. Energy Rev.* **2011**, *15*, 4652–4658. [CrossRef]
6. Tofigh, A.; Abedian, M. Analysis of energy status in Iran for designing sustainable energy roadmap. *Renew. Sustain. Energy Rev.* **2016**, *57*, 1296–1306. [CrossRef]
7. Kaldellis, J.; Vlachou, D.; Korbakis, G. Techno-economic evaluation of small hydro power plants in Greece: A complete sensitivity analysis. *Energy Policy* **2005**, *33*, 1969–1985. [CrossRef]
8. Carapellucci, R.; Giordano, L.; Pierguidi, F. Techno-economic evaluation of small-hydro power plants: Modelling and characterisation of the Abruzzo region in Italy. *Renew. Energy* **2015**, *75*, 395–406. [CrossRef]
9. IEA. *IEA World Energy Balances*; IEA: Paris, France, 2020.

10. Dubey, K.; Dodonov, A. *Mapping of Existing Technologies to Enhance Energy Efficiency in Buildings in the Unece Region*; UNECE: Geneva, Switzerland, 2019.
11. Rezaie, B. Assessing District Energy Systems Performance Integrated with Multiple Thermal Energy Storages. Ph.D. Thesis, Ontario Tech University, Oshawa, ON, Canada, 2013.
12. Collins, J.F. The History of District Heating. *Dist. Heat.* **1959**, *44*, 154–161.
13. Lund, H.; Werner, S.; Wiltshire, R.; Svendsen, S.; Thorsen, J.E.; Hvelplund, F.; Mathiesen, B.V. 4th Generation District Heating (4GDH). Integrating smart thermal grids into future sustainable energy systems. *Energy* **2014**, *68*, 1–11. [CrossRef]
14. Bean, R.; ArchD, K.W.K. Part 1: History of radiant heating & cooling systems. *Ashrae J.* **2020**, *52*, 40.
15. Bean, R.; Olesen, B.W.; Kim, K.W.; Arch, D. Part 2: History of Radiant Heating & Cooling Systems. *Ashrae J.* **2010**, *52*, 50.
16. Sherratt, A.F.C. *Applications of Heat Pumps to Buildings*; Hutchinson: Paris, France, 1987.
17. Yousefi, H.; Abbaspour, A.; Seraj, H. The Role of Geothermal Energy Development on CO_2 Emission by 2030. In Proceedings of the 44th Workshop on Geothermal Reservoir Engineering, Stanford, CA, USA, 11–13 February 2019; pp. 1–6.
18. Gunnlaugsson, E.; Ívarsson, G. Direct Use of Geothermal Water for District Heating in Reykjavík and Other Towns and Communities in SW-Iceland. In Proceedings of the Proceedings World Geothermal Congress 2010, Bali, Indonesia, 25–29 April 2010.
19. Di Lucia, L.; Ericsson, K. Energy Research & Social Science Low-carbon district heating in Sweden—Examining a successful energy transition. *Energy Res. Soc. Sci.* **2014**, *4*, 10–20.
20. Noussan, M.; Abdin, G.C.; Poggio, A.; Roberto, R. Biomass-fired CHP and heat storage system simulations in existing district heating systems. *Appl. Therm. Eng.* **2014**, *71*, 729–735. [CrossRef]
21. Paiho, S.; Saastamoinen, H. How to develop district heating in Finland? *Energy Policy* **2018**, *122*, 668–676. [CrossRef]
22. Lund, H.; Duic, N.; Alberg, P.; Vad, B. Future district heating systems and technologies: On the role of smart energy systems and 4th generation district heating. *Energy* **2018**, *165*, 614–619. [CrossRef]
23. Martin-Du Pan, O.; Eames, P.; Rowley, P.; Bouchlaghem, D.; Susman, G. Current and future operation scenarios for a 50,000 MWh district heating system. *Archit. Eng. Des. Manag.* **2015**, *11*, 280–304. [CrossRef]
24. Lidberg, T.; Gustafsson, M.; Myhren, J.A.; Olofsson, T.; Ödlund, L. Environmental impact of energy refurbishment of buildings within different district heating systems q. *Appl. Energy* **2018**, *227*, 231–238. [CrossRef]
25. Francisco Pinto, J.; Carrilho da Graça, G. Comparison between geothermal district heating and deep energy refurbishment of residential building districts. *Sustain. Cities Soc.* **2018**, *38*, 309–324. [CrossRef]
26. Yousefi, H.; Roumi, S.; Ármannsson, H.; Noorollahi, Y. Cascading uses of geothermal energy for a sustainable energy supply for Meshkinshahr City, Northwest, Iran. *Geothermics* **2019**, *79*, 152–163. [CrossRef]
27. Yıldırım, N.; Gökçen, G. Modeling of Low Temperature Geothermal District Heating Systems. *Int. J. Green Energy* **2004**, *1*, 365–379. [CrossRef]
28. Yildirim, N.; Toksoy, M.; Gokcen, G. Piping network design of geothermal district heating systems: Case study for a university campus. *Energy* **2010**, *35*, 3256–3262. [CrossRef]
29. Blázquez, C.S.; Martín, A.F.; Nieto, I.M.; González-Aguilera, D. Economic and environmental analysis of different district heating systems aided by geothermal energy. *Energies* **2018**, *11*, 1265. [CrossRef]
30. Stegnar, G.; Staničić, D.; Česen, M.; Čižman, J.; Pestotnik, S.; Prestor, J.; Urbančič, A.; Merše, S. A framework for assessing the technical and economic potential of shallow geothermal energy in individual and district heating systems: A case study of Slovenia. *Energy* **2019**, *180*, 405–420. [CrossRef]
31. Chen, Y.; Wang, J.; Lund, P.D. Sustainability evaluation and sensitivity analysis of district heating systems coupled to geothermal and solar resources. *Energy Convers. Manag.* **2020**, *220*, 113084. [CrossRef]
32. Kavian, S.; Hakkaki-Fard, A.; Mosleh, H.J. Energy performance and economic feasibility of hot spring-based district heating system—A case study. *Energy* **2020**, *211*, 118629. [CrossRef]
33. Dahash, A.; Ochs, F.; Janetti, M.B.; Streicher, W. Advances in seasonal thermal energy storage for solar district heating applications: A critical review on large-scale hot-water tank and pit thermal energy storage systems. *Appl. Energy* **2009**, *239*, 296–315. [CrossRef]
34. Renaldi, R.; Friedrich, D. Techno-economic analysis of a solar district heating system with seasonal thermal storage in the UK. *Appl. Energy* **2019**, *236*, 388–400. [CrossRef]
35. Ciapała, B.; Jurasz, J.; Kies, A. The potential of wind power-supported geothermal district heating systems-model results for a location in Warsaw (Poland). *Energies* **2019**, *12*, 3706. [CrossRef]
36. Koch, K.; Matthias, G. Intelligent Controling of Power Driven Solid Biomass CHP Plants in Flexible District Heating with a Seasonal Heat Storage and a Power-to-Heat Component. In Proceedings of the 26th European Biomass Conference and Exhibition, Copenhagen, Denmark, 14–17 May 2018; ETA-Florence Renewable Energies: Firenze, Italy, 2018; pp. 14–17.
37. Rastegarpour, S.; Ferrarini, L.; Palaiogiannis, F. A Distributed Predictive Control of Energy Resources in Radiant Floor Buildings. *J. Dyn. Syst. Meas. Control.* **2019**, *141*, 101013. [CrossRef]
38. Zhou, G.; He, J. Thermal performance of a radiant floor heating system with different heat storage materials and heating pipes q. *Appl. Energy* **2015**, *138*, 648–660. [CrossRef]
39. Østergaard, P.A.; Jantzen, J.; Marczinkowski, H.; Kristensen, M. Business and socioeconomic assessment of introducing heat pumps with heat storage in small-scale district heating systems. *Renew. Energy* **2019**, *139*, 904–914. [CrossRef]
40. Noorollahi, Y.; Yousefi, H.; Itoi, R.; Ehara, S. Geothermal energy resources and development in Iran. *Renew. Sustain. Energy Rev.* **2009**, *13*, 1127–1132. [CrossRef]

41. Del, F.; Gonzalo, A.; Ferrandiz, J.A. Building Energy Modeling by means of BIM software. A case study with Water Flow Glazing. In Proceedings of the Seventh European Conference on Renewable Energy Systems (ECRES2019), Madrid, Spain, 10–12 June 2019.
42. Krawczyk, D.A. Analysis of Energy Consumption for Heating in a Residential House in Poland. *Energy Procedia* **2016**, *95*, 216–222. [CrossRef]
43. Yin, C.; Rosendahl, L.A.; Kær, S.K. Grate-firing of biomass for heat and power production. *Prog. Energy Combust. Sci.* **2008**, *34*, 725–754. [CrossRef]
44. Weather Data. EnergyPlus. Available online: https://energyplus.net/weather (accessed on 28 September 2022).
45. ASHRAE. *ASHRAE Handbook—HVAC Systems and Equipment*; American Society of Heating, Refrigerating and Air-Conditioning Engineers: Atlanta, GA, USA, 2000.
46. Arkay, K.E.; Blais, C. *The District Energy Options in Canada*; Natural Resources Canada: Bonnyville, AB, Canada, 1999.
47. Schweitzer, J. *Full and Part Load Efficiency Measurements for Boilers*; Office of Energy Efficiency and Renewable Energy: Washington, DC, USA, 1996.
48. Satyavada, H.; Baldi, S. Monitoring energy efficiency of condensing boilers via hybrid first-principle modelling and estimation. *Energy* **2018**, *142*, 121–129. [CrossRef]
49. Rafferty, K.D.; Culver, G. Heat exchangers. In *Geothermal Direct Use Engineering and Design Guidebook*; USDOE: Washington, DC, USA, 1998.
50. Vallios, I.; Tsoutsos, T.; Papadakis, G. Design of biomass district heating systems. *Biomass Bioenergy* **2009**, *33*, 659–678. [CrossRef]
51. Tchobanoglous, G.; Theisen, H.; Vigill, S. *Integrated Solid Waste Management: Engineering Principles and Management Issues*; Tsinghua University Press: Beijing, China, 1993.
52. AEA. *Waste Management Options and Climate Change*; AEA: Nashville, TN, USA, 2001.
53. Teichmann, D.; Schempp, C. *Calculation of GHG Emissions of Waste Management Projects*; JASPERS Knowledge Economy and Energy Division: Brussels, Belgium, 2013.
54. Pipatti, R.; Sharma, C.; Yamada, M.; Alves, J.W.S.; Gao, Q.; Guendehou, G.H.S.; Cabrera, M.; Mareckova, K.; Oonk, H.; Scheehle, E.; et al. Waste Generation, Composition and Managment Data. In *2019 Refinement to the 2006 IPCC Guidelines for National Greenhouse Gas Inventories*; Chapter 2; IPCC: Geneva, Switzerland, 2006.
55. Nowrouzi, A.; Panahi, M.; Ghaffarzadeh, H.; Ataei, A. Optimizing Iran's natural gas export portfolio by presenting a conceptual framework for non-systematic risk based on portfolio theory. *Energy Strateg. Rev.* **2019**, *26*, 100403. [CrossRef]